Applied Physics A (2020) 126:145
https://doi.org/10.1007/s00339-020-3331-0

Applied Physics A
Materials Science & Processing

A novel synthesis and characterization of transparent CdS thin films for CdTe/CdS solar cells

Md.Ferdous Rahman[1,2] · Jaker Hossain[1] · Abdul Kuddus[1,5] · Samia Tabassum[3] · Mirza H. K. Rubel[4] · Hajime Shirai[5] · Abu Bakar Md. Ismail[1]

Received: 3 January 2020 / Accepted: 20 January 2020

Abstract

We demonstrate the direct synthesis of CdS thin films by spin coating method with thiol-amine co-solvents system. Annealing of the films at various temperatures has been performed in the air using simple glass protector. The XRD patterns show a strong peak along (110) plane related to cubic lattice while two weak peaks at (002) and (100) planes indicate the hexagonal symmetry for the CdS thin films. The Raman peak at 305 cm^{-1} also confirms the formation of crystalline CdS thin films. The FTIR study also reveals the formation of CdS thin films. The SEM images reveal the surface uniformity and homogeneity of the CdS thin films. The EDX results indicate nearly stoichiometric CdS thin films. The optical band gap of CdS thin films is ~ 2.4 eV when coated at 2000 rpm and annealed at 300 °C for 5 min. These findings indicate that synthesized CdS films are potential candidates for solution-processed CdTe/CdS solar cells.

Keywords CdS thin film · CdTe/CdS solar cell · Spin coating · Thiol-amine co-solvent · Transparent

1 Introduction

The highly competitive cadmium telluride (CdTe) thin film solar cells (TFSCs) are hopeful candidates to the photovoltaic (PV) research community due to the highest power conversion efficiency (PCE) of 22.1% and an open-circuit voltage (OCV) greater than 1 V [1–3]. The comparable emission of pollutants with silicon (Si) PV and notably alleviated emissions with sources of fossil energy materials have motivated the fabrication of high throughput low-cost solution-processed CdTe based solar cells [4, 5]. Generally, alloy compounds poses low resistance to the aggressive influence of environmental factors such as temperature, oxygen and electromagnetic radiation compared with the oxide compounds like iron oxides particularly the hexaferrites which are a promising complex for practical use as semiconductors shows more stability when used as dielectrics up to 1000 °C [6, 7]. Among other compounds, cadmium sulfide (CdS) possesses low resistivity and high transmittance, therefore PV researchers consider it as one of the most extensively utilized n-type window materials for the CdTe TFSCs [8–10]. In addition, it is widely used in light emitting diodes (LEDs) [11] and transistors [12]. At room temperature (RT), the direct energy band gap of CdS is about 2.42–2.5 eV. The CdS thin films can be effectively grown in both zinc blende (cubic) as well as wurtzite (hexagonal) phases [13]. Regarding the appropriate PV applications, a good number of researches have been carried out for producing the CdS thin films that could offer improved optoelectronic properties like relatively higher transparency

Electronic supplementary material The online version of this article (https://doi.org/10.1007/s00339-020-3331-0) contains supplementary material, which is available to authorized users.

✉ Jaker Hossain
jak_apee@ru.ac.bd

✉ Abu Bakar Md. Ismail
ismail@ru.ac.bd

[1] Solar Energy Laboratory, Department of Electrical and Electronic Engineering, University of Rajshahi, Rajshahi 6205, Bangladesh

[2] Department of Electrical and Electronic Engineering, Begum Rokeya University, Rangpur, Rangpur 5400, Bangladesh

[3] Institute of Fuel Research and Development, Bangladesh Council of Scientific and Industrial Research, Dhaka 1205, Bangladesh

[4] Department of Materials Science and Engineering, University of Rajshahi, Rajshahi 6205, Bangladesh

[5] Graduate School of Science and Engineering, Saitama University, Saitama 338-8570, Japan

Published online: 01 February 2020

as well as greater photoconductivity to reduce the electrical losses [14]. Recently, CdS thin films have been fabricated by varieties of deposition methods including the chemical vapour deposition (CVD) [15], the physical vapour deposition (PVD) [16], the metal–organic CVD (MOCVD) [17], the chemical bath deposition (CBD) [18, 19], sol–gel [20], spray pyrolysis [21], the molecular beam epitaxy (MBE) [22], pulsed electrolyte deposition [23–25], electrochemical deposition [26, 27], electrodeposition [28, 29] etc. However, these methods always involve expensive equipments and a special protective environment together with strict operational conditions. Other than the above mentioned techniques, emerging potential techniques such as the successive ionic layer adsorption and reaction (SILAR) and the Langmuir–Blodgett (LB) methods have been developed for forming CdS nanoparticles [30, 31].

Nowadays, the thiol-amine universal solvent system has emerged as a potential system for the solution-processed fabrication of first-class films of V_2VI_3 (V = As, Bi, Sb; VI = Te, Se, S) semiconductors, tin sulphide (SnS), CdTe and other chalcogenide materials potential for solar cell applications [5, 32–34]. More recently, some effective citrate sol–gel methods have been developed to obtain solution-processed complex compounds [35, 36]. So far, spin coated CdS films have been produced dissolving the metal-oxides, -hydroxides, -chlorides, -acetyl acetonates and -acetates in thioglycolic acid and ethanol-amine, respectively employing the sophisticated inert annealing system [37]. However, we can hardly find any literature reporting the synthesis of CdS films with the thiol-amine solvent system directly dissolving CdS source materials.

In this current work, we have fruitfully synthesized CdS thin films by a conventional simple spin coating method incorporating a novel thiol-amine solvent system containing 1,2-ethylene-di-amine (en) and 1,2-ethane-di-thiol ($edtH_2$), respectively. This scheme can simply be practiced for large-scale deposition of CdS thin films. We characterized the synthesized CdS thin films by the X-ray diffraction (XRD) technique, the scanning electron microscopy (SEM), the Raman and the Fourier-transform Infra-red (FTIR) Spectroscopies for investigating the phases, local structures, microstructures, and surface morphology in detail to reveal their suitability for CdTe/CdS solar cells.

2 Experimental details

2.1 Preparation of precursor solution

CdS powder (99.9999%), ethylene-di-amine, 1,2 ethane-di-thiol and Triton X-100 purchased from Sigma Aldrich were used to prepare CdS solution without further purifications. Firstly, ethylene-di-amine and 1,2 ethane-di-thiol were mixed at a volume ratio of 10:1 and then 0.3 wt% CdS powder was dissolved in the mixed co-solvents. The colour of the solution was yellow. Then the solution was stirred for 15 h at 50 °C temperature in a magnetic stirrer to completely dissolve the CdS powder. After stirring, the solution was optically transparent and very faint yellow in colour as shown in Fig. 1. After that a small amount of Triton X-100 surfactant (< 0.1 wt%) was added in the solution to make uniform and high quality CdS thin films.

2.2 Deposition of CdS thin films

The CdS thin film was deposited using the spin coating method on to glass substrate (2×2 cm^2) using the prepared CdS dissolved thiol-amine solution. The glass substrates were first cleaned with piranha solution to remove gross contamination [38]. Before film deposition, the glass substrate was cleaned using acetone, IPA and DI water each for 10 min and dried by an air blower.

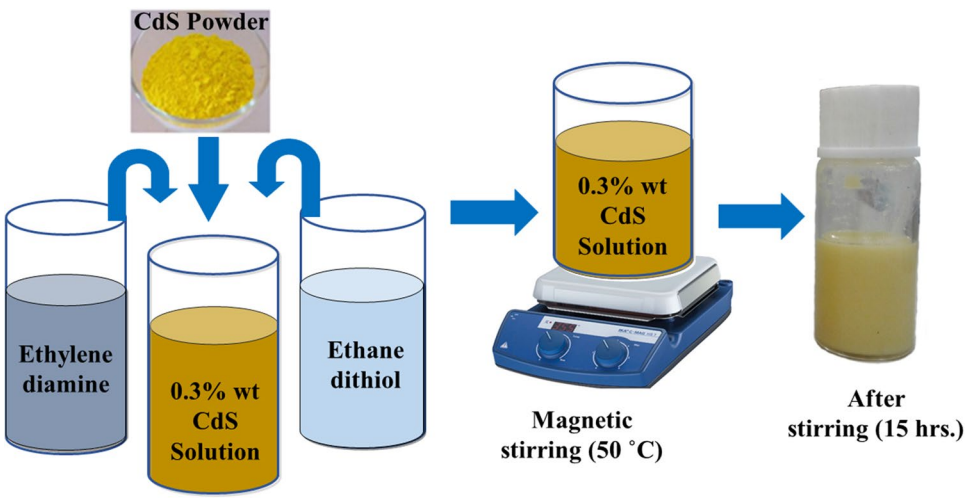

Fig. 1 Preparation of 0.3 wt% CdS solution using thiol-amine co-solvents with surfactant for CdS thin films

The CdS precursor solution was spin coated one time on cleaned substrates at speeds of 1000, 1500, and 2000 rpm, respectively for 45 s. Then the deposited CdS films were dried at 90 °C at 10 min on a hot plate to take away the remaining solvents, which we called pre-annealing process. Then the pre-annealed CdS films were annealed in the air with glass protector at high temperatures and times for 250–350 °C and 3–7 min respectively for the crystallization of the films [22]. The high temperature annealing was performed in a carbolite oven using glass protector (fastened with stainless steel clip) system to avoid oxidation of the films. The variation of the thicknesses of the corresponding films is shown in figure S1 in the supporting information. The substrate cleaning, deposition, and annealing process of CdS thin films are depicted in Fig. 2.

2.3 Characterization of CdS thin films

The BRUKER DekTak XTL thickness profiler was used to measure the synthesized CdS film thickness. The structure of CdS thin films was characterized by XRD using the CuKα radiation (wavelength, $\lambda = 1.5418$ Å). To understand and explore the molecular arrangements and local structure of the CdS thin films, the micro-Raman measurement was also carried out using an excitation wavelength of 532 nm of the neodymium-doped yttrium aluminium garnet (Nd:YAG) laser (inVia, Renishaw) having 800 lines/mm grating, charge coupled device (CCD) detector of 1.4 cm^{-1}/pixel and Eclipse notch filter. The FTIR spectra were also recorded in the wavenumber range of 400–4000 cm^{-1} to further understand the local structure of CdS thin films. The morphological analysis was performed by means of SEM (Carl Zeiss, Model: EVO-18 Research). The EDX analysis was carried out to detect the constituent elements of CdS thin films with an energy dispersive X-ray spectroscopy (EDX) detector linked to SEM equipment. The optical characterization was conducted carefully using a T-60 ultraviolet–visible (UV–Vis) spectrophotometer (PG Instruments) by determining the films' transmission spectra in the wavelength range of 360–1100 nm.

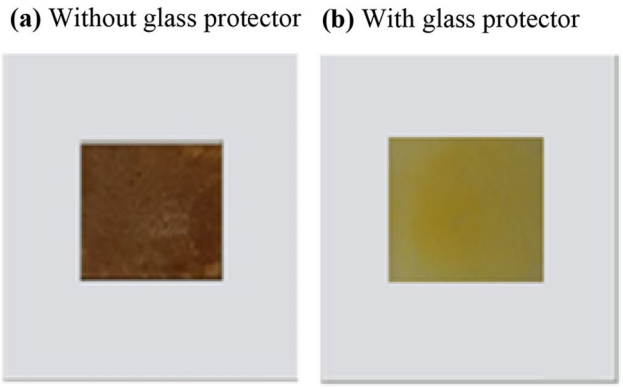

Fig. 3 The optical images of the CdS films annealed at the temperature of 250 °C with and without glass protector in carbolite oven

3 Results and discussion

3.1 Annealing effect on CdS thin films

So far, annealing of the films deposited with thiol-amine co-solvents is performed in an inert environment to avoid oxidation [5, 32]. Here, in this study, annealing has been performed in air using a different approach as shown in Fig. 2. Since use of inert environment is expensive than open air, the glass protector was used to avoid oxidation that offers very low cost and very simple way for avoiding the oxidation of the film instead of the sophisticated inert annealing system as shown in the figure. The glass protector was fastened with stainless steel clip implying a protection system that could avoid oxidation of the films when annealed at temperatures till 300 °C for not more than 5 min. The avoidance of oxidation can be confirmed from the EDX analysis discussed

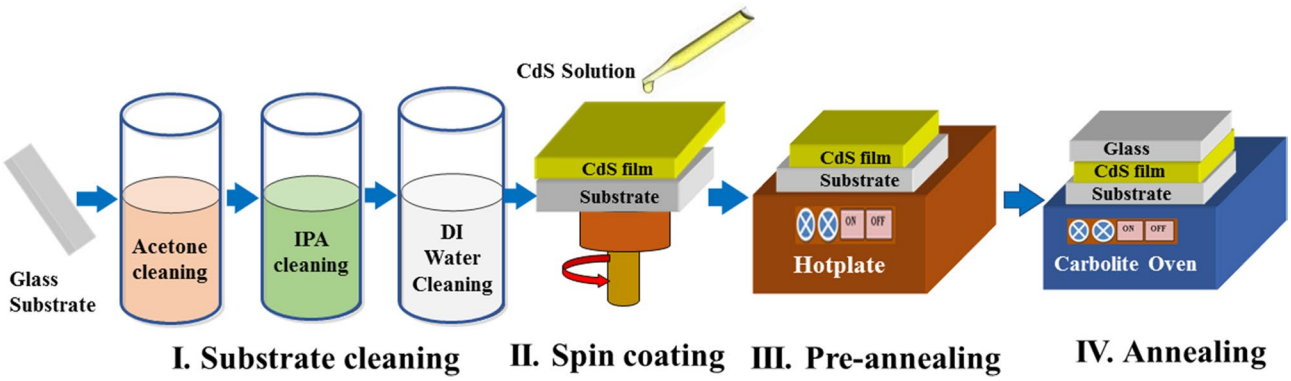

Fig. 2 Substrate cleaning, deposition and annealing steps for CdS thin films using the spin coating method with glass protector

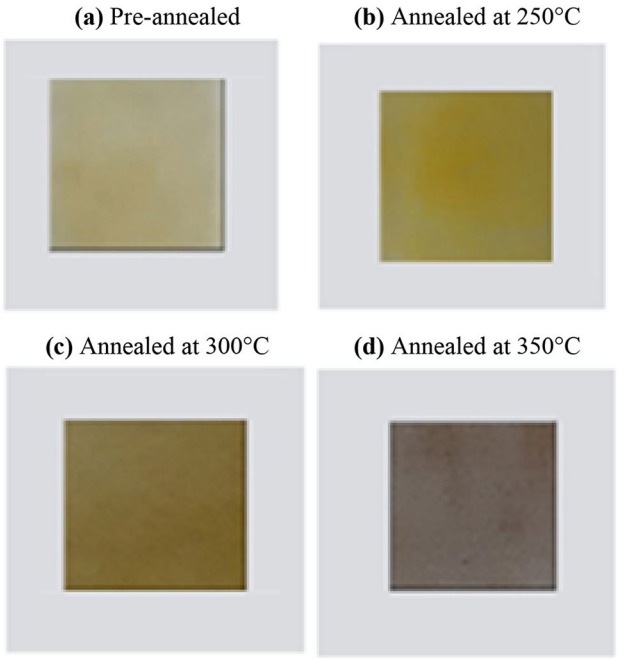

Fig. 4 The optical images of CdS films annealed at different temperatures for 5 min

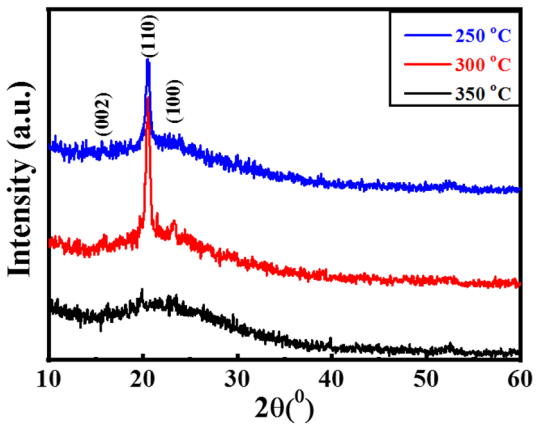

Fig. 5 The XRD spectra of CdS films spin coated at 2000 rpm using thiol-amine co-solvents

in a later Sect. 3.2.5. Air annealing drastically changes the CdS thin films' colour to faint black whereas the colour of the film remains yellow when a glass protector is used on the top of the film as shown in Fig. 3. This figure indicates that oxidation of the film can be restrained using glass protector.

Figure 4a–d show the optical images of the CdS thin films deposited at 2000 rpm and annealed for 5 min at different temperature using glass protector. As shown in Fig. 4a, the color of the pre-annealed CdS film is relatively white yellow. The films annealed at 250 °C temperature appear as faint yellow and that annealed at 300 °C is yellow. The CdS thin film annealed at 350 °C the film looks faint black which indicates that glass protector cannot restrict oxidation over 300 °C. Figure S2 also shows the color of the deposited CdS thin films annealed at 300 °C for various times. It is shown from the figure that glass protector cannot suppress oxidation also for annealing time over 5 min.

3.2 Structural studies of CdS thin films

3.2.1 X-ray diffraction (XRD) study

The XRD patterns of synthesized CdS thin films at 2000 rpm and annealed at temperatures of 250 °C, 300 °C, and 350 °C are depicted in Fig. 5. It is evident from the spectra that there is a main peak, originated at $2\theta = 20.5°$, which corresponds to the cubic structure of the films with lattice parameter, $a = 5.82$ Å and preferential orientation along (110) plane [39–41]. This peak with cubic structure mainly arises when CdS is synthesized from $CdSO_4$ source materials [40, 41]. There are also some reports where it is believed that this peak arises due to the influence of oxygen [42, 43]. The CdS thin films were fabricated in this study with no sulphate source and annealing was performed with glass protector in the air. Therefore, oxygen might have an indirect effect for the crystal formation at this 2θ values as there is a possibility to ingress oxygen during annealing process, although oxygen was not detected from EDX study as will be discussed later. It is also observed from Fig. 5 that with annealing temperature the intensity of this peak changes and the highest intensity reaches for 300 °C whereas it diminishes for 350 °C which indicate that annealing temperature has significant influence on crystallization of the film. In fact, no peaks were detected for higher annealing temperatures indicating the amorphous nature of the film. There are also two weak peaks that emerge at ~ $2\theta = 15.5°$ and 23.1° for annealing temperature of 300 °C has the hexagonal structure with (002) [44] and (100) planes [39], respectively.

The CdS thin film deposited by this easy means with suitable annealing temperature of 300 °C reveals the formation of high-quality films due to the absence of impurity peaks [45]. To acquire information about the lattice parameters, the crystallinity levels, the full width at half maximum (FWHM), the crystallite size (D), dislocation density (δ) were computed from the obtained XRD data.

The crystallite size, D can be estimated using Scherrer's equation (1) [46, 47],

$$D = \frac{0.9\lambda}{\beta\cos\theta}, \tag{1}$$

where, λ is the wavelength of the X-ray in nm, β is the FWHM of the peak in radians and θ is the Bragg angle of the related peak.

The dislocation density, δ was calculated as given by Eq. (2) for various peaks of the CdS films [48],

$$\delta = 1/D^2. \quad (2)$$

The calculated crystallite sizes at planes 110 and 100 were about 71.45 and 71.8 nm, respectively and the dislocation densities of the corresponding crystallites were about 1.96×10^{14} and 1.94×10^{14} lines/m^2, respectively for the film annealed at 300 °C. Therefore, we can conclude that the CdS films fabricated by this simple thiol-amine solution-process showed good crystallinity.

However, annealing temperature affects the electronic properties as well as mass transport and the grain boundaries of the films. The change of crystallite size of deposited films reflects the impact of annealing temperature on these properties. It is found that with the increasing annealing temperature, the crystallite size increases and also the crystal structure and electromagnetic properties of the films are affected by annealing temperature [49, 50]. A similar result was also observed for the CdS thin films synthesized by CBD method where D increases and δ decreases with an increase in the annealing temperature [51].

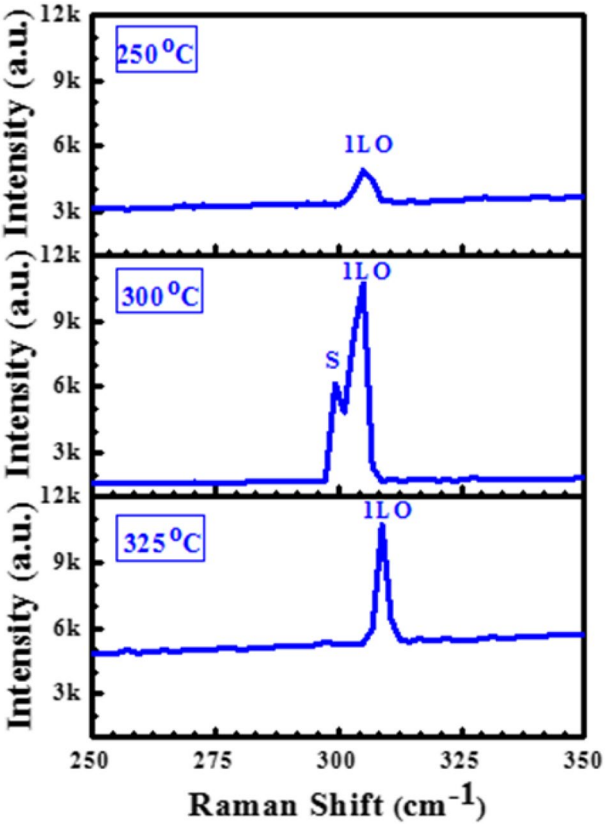

Fig. 6 Raman spectra of CdS films deposited at 300 °C and annealed at different temperatures for 5 min

3.2.2 Raman analysis of CdS thin films

Figure 6 delineates the RT (~ 300 K) Raman spectra of CdS thin films spin coated at 2000 rpm and annealed at diverse temperatures for 5 min. It is revealed from the figure that the first order longitudinal optical (1LO) Raman peak appears at 305 cm^{-1} wave number for the film annealed at 300 °C, which agrees well with the reported value [52, 53]. Another shoulder peak (*S*) also observed at 300 cm^{-1} which may be attributed to the surface phonon mode of the film as shown in the Fig. 6 [54]. It can be seen from the figure that 1LO peak shifts to lower and higher frequency for the variation of annealing temperature from 250 to 325 °C, respectively. It is interesting to note that the intensity of the 1LO Raman peak is higher for the film annealed at 300 °C which decreases when annealed at temperatures of 250 °C and 325 °C, respectively. The change in frequency and peak intensity with annealing temperature are depicted in figure S3 in the supporting information. These shifts in frequency and peak intensity may be attributed due to crystallite size effect or surface phonon mode effect or the mechanical stress in the interface [55, 56]. Therefore, it can be concluded from the Raman data that 300 °C is the favorable temperature for the growth of spin coated and air-annealed CdS thin film using thiol-amine co-solvents. This is also consistent with the XRD data, which indicate that CdS thin films annealed at 300 °C has the highest peak intensity.

3.2.3 The FTIR study of CdS thin films

The FTIR spectra were recorded to further realize the local structure and bonding of the CdS films synthesized in the present work. Figure 7 delineates the FTIR spectra of CdS films in the range of 400–4000 cm^{-1} at different

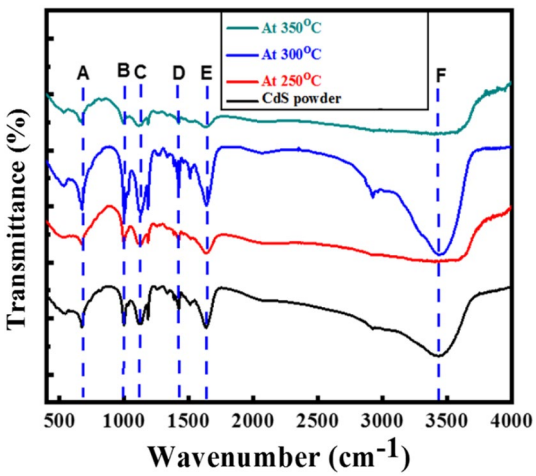

Fig. 7 FTIR spectra of CdS films synthesized by spin coating at 2000 rpm using thiol-amine co-solvents system

Table 1 The FTIR peak assignment of spin coated CdS films at 2000 rpm using thiol-amine co-solvents

Peak's symbol	Wavenumber (cm^{-1})	Intensity	Bond types	References
A	670–675	Sharp and strong	Cd–S stretching	[57]
B	995–1001	Sharp	C–O stretching	[58]
C	1180–1185	Small and weak	C–O–C stretching	[59]
D	1420–1423	Small and weak	C–H bending	[60]
E	1630–1635	Sharp and broad	O–H bending	[61]
F	3400–3435	Broad	O–H stretching	[61]

temperatures and spin coated at 2000 rpm. Figure 7 also shows the FTIR spectra of CdS source powder. Symbols '*A*' to '*F*' in Fig. 7 indicates the corresponding peaks of different functional groups present in the films and are also listed in Table 1. The band of absorption (670–675 cm^{-1}) labelled as '*A*' is due to the Cd–S bonding which agrees well with reported value [57]. It is also seen from the figure that the peak intensity of this band is higher for the film annealed at 300 °C. The C–O stretching vibration (*B*) of absorbed CO_2 gives its intense sharp peak at 995–1001 cm^{-1} [58]. The small and weak peak due to C–O–C stretching is observed at absorption band 1180–1185 cm^{-1} [59]. The presence of a small and weak absorption peak at band 1420–1423 cm^{-1} is attributed to C–H bending [60]. The band of absorption (1630–1635 cm^{-1}) labelled as '*E*' is due to the O–H bending vibration of water molecule [61]. A large absorption broad peak corresponding to 3400–3435 cm^{-1} is arising due to the O–H group shows the extending vibration of the absorbed H_2O on the CdS surface [61]. It is interesting to note from the figure that both (*E*) and (*F*) peaks are pronounced like those of CdS powder for the film annealed at 300 °C indicating the optimal temperature for the growth of CdS thin film as also confirmed by XRD and Raman studies.

3.2.4 SEM study of CdS thin films

The CdS films' surface morphology was explored using SEM. Figure S4(a) and S4(b) delineate the surface morphologies of CdS films without and with Triton X-100 surfactant, respectively. It is observed from the figure that the CdS films' surfaces become uniform and smooth with the addition of surfactant in the CdS- dissolved thiol-amine solution. Figure 8 depicts the SEM images of spin coated CdS thin films at 2000 rpm using thiol-amine co-solvents at different magnifications. The obtained results confirm that the CdS film surface is uniform, dense as well as homogeneous having less pinholes or cracks compared to that of the sophisticated methods of CdS thin film deposition [62].

3.2.5 The EDX study of CdS thin films

The stoichiometry is an important property for compounds. The deviation of the concentration of the original cations from a specified value can lead variation in the charge state of the cations, which in turn will greatly change the electronic properties of that compound thereafter affect the practical application of the deposited thin films [63, 64]. The EDX analysis was performed to inspect the elemental composition of the CdS thin films. This measurement was performed at different spots to determine the precise compositions. Figure S5 shows the EDX spectrum of CdS coated 2000 rpm and annealed at 300 and 350 °C, respectively. The EDX elemental composition of CdS films confirm the existence of Cd and S elements and are presented with error scale in Table 2. It ensures that the CdS thin films comprise the elements cadmium (Cd) and sulphur (S) and the atomic % ratio of the film is nearly 1 when annealed at 300 °C. The film is oxidized when the annealing temperatures exceed this temperature as shown in the table which may have happened due to the fact that the glass protector cannot restrain oxidation of the films at high temperatures. Therefore, it can be inferred that the deposited CdS thin films using thiol-amine co-solvents at 300 °C are approximately stoichiometric with slightly S rich, which is consistent with that of the other solution-processed methods [65]. No other elements were detected in the deposited films. This indicates the development of high quality CdS thin films. However, the relatively small error in atomic percentages in Table 2 can be ascribed to non-quantitative measurement of CdS thin films.

3.3 Optical properties of CdS thin films

3.3.1 Annealing effect on transmittance of CdS thin films

Figure 9 shows the annealing effect on the transmittance of CdS thin films prepared by spin coating at 2000 rpm using thiol-amine co-solvents. Figure 9a demonstrates the annealing temperature effect on the transmittance of CdS thin films along with transmittance of pre-annealed film including base

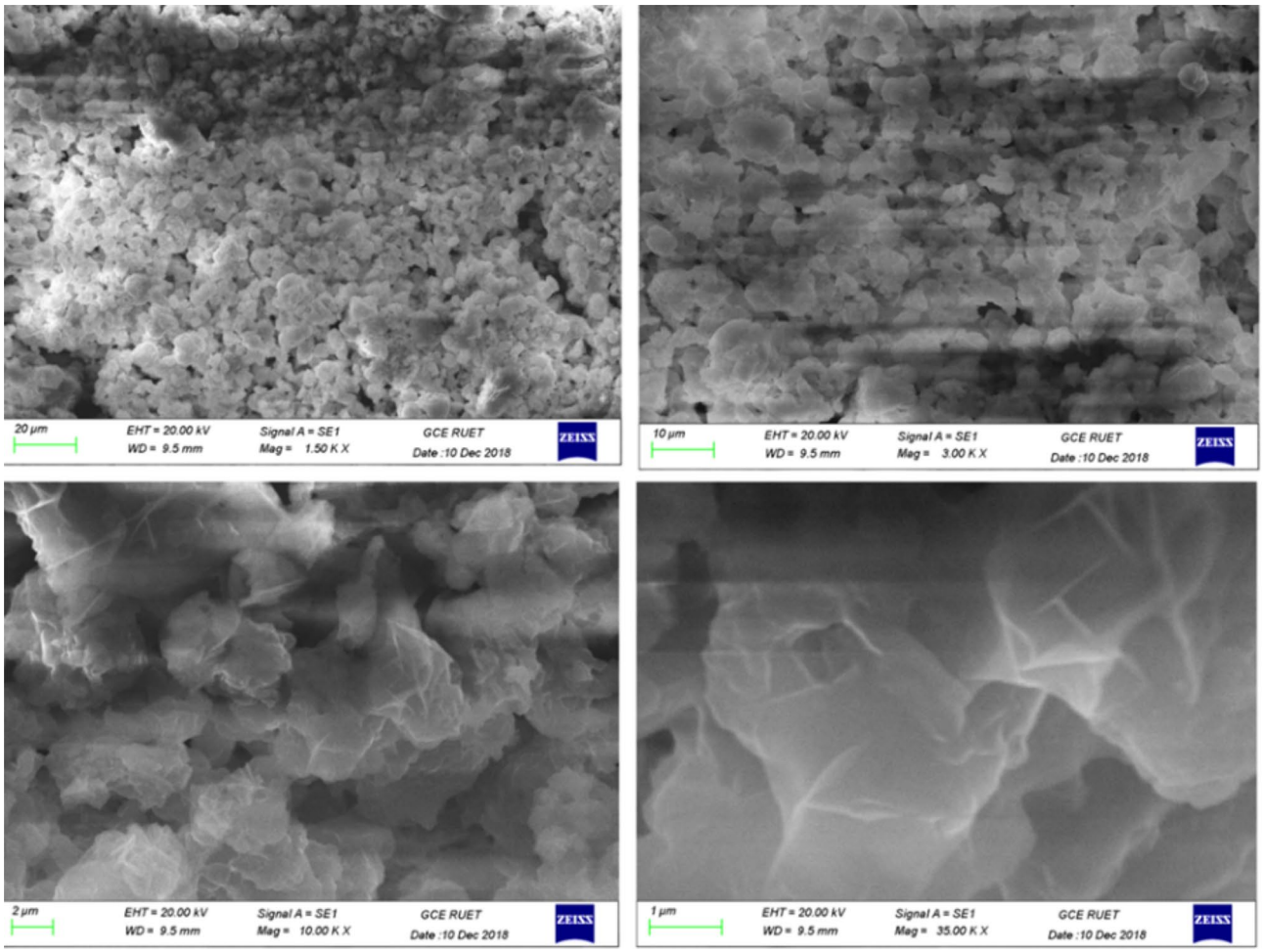

Fig. 8 The SEM images at different magnifications of CdS films for annealing temperature and time of 300 °C and 5 min, respectively

Table 2 The EDX elemental composition of CdS thin films spin coated at 2000 rpm and annealed at 300 and 350 °C, respectively with error scale

Annealing temperature (°C)	Elements	Weight%	Atom%	Atomic error (%)
300	S	53.63	52.97	±0.30
	Cd	46.37	47.03	±0.22
	Total	100	100	
350	S	44.63	41.97	±0.33
	Cd	37.07	38.93	±0.27
	O	18.30	19.10	±0.10
	Total	100	100	

line correction of bare glass substrate. Pre-annealed samples show the transmittance of ~ 30–40%. But when the films are annealed at 250 °C, 300 °C, and 350 °C for 5 min, the transmittance of the films increases to 60–65%, 80–85% and 50–55%, respectively. The film showed the highest transmittance was annealed at 300 °C, but transmittance decreases when the annealing temperature is either low or high. This is because of the fact that the crystallization as well as oxidation of the films depends on annealing temperature as shown in Figs. 4 and 5, respectively.

Figure 9b shows the consequence of annealing time on the transmittance of the CdS thin films annealed at 300 °C. The film annealed for 5 min shows the highest transmittance. The transmittance decreases for the films annealed for 3 or 7 min. This happens due to the fact that the destruction of crystal quality and oxidation occur at the film as glass protector cannot restrict oxidation for a long time which results in black colouring of the CdS thin films as shown in figure S2 in the supporting information. The change of transmittance of the CdS films with spin coating speed is also shown figure S6. It is seen from the figure that transmittance increases with rpm increment, which is consistent as thickness of the film decreases with the rpm which results in increase in transmittance. Therefore, it can be concluded that the optimum condition for

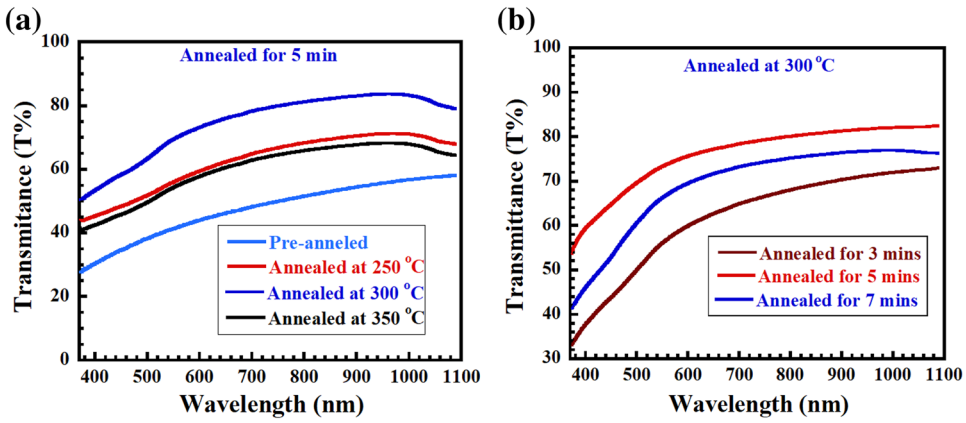

Fig. 9 The transmittance spectra of CdS thin films synthesized at 2000 rpm and annealed at different **a** temperatures and **b** time

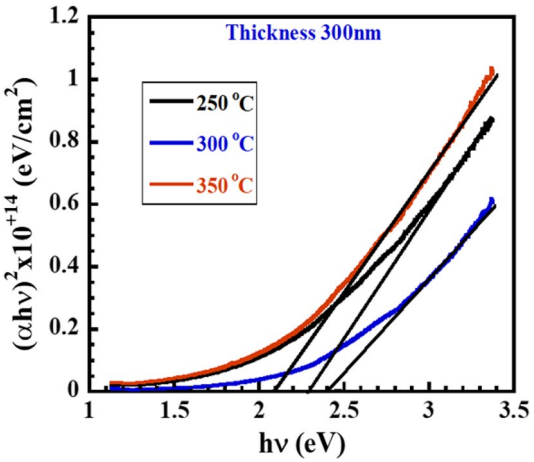

Fig. 10 The plot of $(\alpha h\nu)^2$ versus photon energy $(h\nu)$ for CdS thin-films coated at 2000 rpm and annealed at three different temperatures

transmittance is at spin coating speed of 2000 rpm and an annealing temperature of 300 ℃ for 5 min.

When the wavelengths were below 550 nm, the CdS film's transmittance decreases rapidly. It must be written here that high transmittance in the visible area is one of the key attributes for window films in heterojunction solar cells. From the transmittance (T) spectra in the strong absorption zone, we calculated the absorption coefficient (α) as given by the following Eq. (3),

$$\alpha = \frac{\ln\left(\frac{100}{T}\right)}{d}, \tag{3}$$

where, the transmittance and film thickness are denoted by 'T' and d (=300 nm), respectively.

The CdS thin films offer low absorption and high transmittance in the wavelength, $\lambda > 550$ nm, making these films proper window materials in the solar cells. CdS materials have direct band gap. So, as illustrated in Fig. 10, the band energy, E_g of the CdS thin films was evaluated directly by extrapolating the linear segment of $(\alpha h\nu)^2$ versus photon energy $(h\nu)$ plot to $\alpha = 0$.

The obtained value of E_g is 2.4 eV for the CdS film annealed at 300 °C, which has good conformity with the reported experimental values [66, 67]. As seen from the same figure, the CdS thin films annealed at 250 °C and 350 °C have the band gap of 2.3 eV and 2.1 eV, respectively. The decrease in the band gap below 300 °C can be attributed due to unstructured crystal defects which may introduce additional energy levels below the conduction band edge resulting in the reduction of band gap [68]. And also, the reduction in band gap above 300 °C may be explained with the hypothesis that high temperature annealing may cause oxidation of the film forming cadmium oxide (CdO), which has a band gap of the order of 2.16 eV [67, 69]. These results indicate that the synthesized CdS thin films are potential candidate for the fabrication of CdTe/CdS solar cells. In fact, our recent report of SCAPS-1D simulation using experimental data of various parameters of the synthesized CdS thin film reveal the encouraging efficiency of 19.58% and 23.50% (without and with EB-HTL) of the CdTe/CdS solar cells [70].

4 Conclusion

We report the successful synthesis of CdS thin films in air by spin coating method incorporating thiol-amine solutions. The synthesized films were analysed by XRD, SEM, EDX Raman, and FTIR characterization techniques. The XRD results indicate the growth of high quality CdS thin films with the existence of both cubic and hexagonal phases at 300ºC. The Raman and FTIR studies reveal the growth of high quality CdS thin films at 300 °C which supports the XRD patterns as well. The SEM images depict that the CdS film surface is homogeneous and smooth. The EDX results indicate that the fabricated CdS thin film is nearly stoichiometric with slightly

S rich. The optical band gap of CdS thin films is ~ 2.4 eV with higher transmittance. These findings indicate the potentiality of the use of CdS thin films for an efficient solution processed CdTe/CdS solar cells in near future.

Acknowledgements This study was partially supported by a Grant (#BS-159, 2017) from the Ministry of Science & Technology, Govt. of Bangladesh. The authors highly appreciate Mr. Yuma Moriya, Graduate School of Science and Engineering, Saitama University, Japan for helping with the Raman measurement. The authors are also indebted to Mr. Md. Saiduzzaman, Center for Crystal Science and Technology, University of Yamanashi, Japan for his help during the XRD analysis.

Compliance with ethical standards

Conflict of interest The authors declare that they have no conflict of interest.

References

1. A.G. Martin, E. Keith, H. Yoshihiro, W. Wilhelm, Solar cell efficiency tables (version 45). Prog. Photovolt. **23**, 1–9 (2015). https://doi.org/10.1002/pip.2573
2. J.M. Burst, J.N. Duenow, D.S. Albin, E. Colegrove, M.O. Reese, J.A. Aguiar, C.S. Jiang, M.K. Pate, M.M. Al-Jassim, D. Kuciauskas, S. Swain, T. Ablekim, K.G. Lynn, W.K. Metzger, CdTe solar cells with open-circuit voltage breaking the 1 V barrier. Nat. Energy. **1**, 16015 (2016). https://doi.org/10.1038/NENERGY.2016.15
3. M.H. Ali, M.M.A. Moon, M.F. Rahman, Study of ultra-thin CdTe/CdS heterostructure solar cell purveying open-circuit voltage ~ 1.2 V. Mater. Res. Express **6**, 095515 (2019). https://doi.org/10.1088/2053-1591/ab3089
4. V.M. Fthenakis, H.C. Kim, E. Alsema, Emissions from photovoltaic life cycles. Environ. Sci. Technol. **42**, 2168–2174 (2008). https://doi.org/10.1021/es071763q
5. C.K. Miskin, A. Dubois-Camacho, M.O. Reese, R. Agrawal, A direct solution deposition approach to CdTe thin films. J. Mater. Chem. C **4**, 9167–9171 (2016). https://doi.org/10.1039/C6TC02986H
6. A.V. Trukhanov, V.G. Kostishyn, L.V. Panina, V.V. Korovushkin, V.A. Turchenko, P. Thakur, A. Thakur, Y. Yang, D.A. Vinnik, E.S. Yakovenko, L.Y. Matzui, E.L. Trukhanova, S.V. Trukhanov, Control of electromagnetic properties in substituted M-type hexagonal ferrites. J. Alloys Compd. **754**, 247–256 (2018). https://doi.org/10.1016/j.jallcom.2018.04.150
7. S.V. Trukhanov, A.V. Trukhanov, L.V. Panina, V.G. Kostishyn, V.A. Turchenko, E.L. Trukhanova, A.V. Trukhanov, T.I. Zubar, V.M. Ivanov, D.I. Tishkevich, D.A. Vinnik, S.A. Gudkova, D.S. Klygach, M.G. Vakhitov, P. Thakur, A. Thakur, Y. Yang, Temperature evolution of the structure parameters and exchange interactions in $BaFe_{12-x}In_xO_{19}$. J. Magn. Magn. Mater. **466**, 393–405 (2018). https://doi.org/10.1016/j.jmmm.2018.07.041
8. J. Patel, F. Mighri, A. Ajji, D. Tiwari, T.K. Chaudhuri, Spin-coating deposition of PbS and CdS thin films for solar cell application. Appl. Phys. A **117**, 1791–1799 (2014). https://doi.org/10.1007/s00339-014-8659-x
9. K.L. Chopra, S.R. Das, *Thin Films Solar Cells*, vol. 424 (Springer, New York, 1983). https://doi.org/10.1007/978-1-4899-0418-8
10. K.W. Mitchell, C. Eberspecher, J. Enmer, D. Pier, in *Proceedings of 20th IEEE Photovoltaîc SPI Conference 1989, IEEE ISC, 1384* (1989)
11. P. Rastogi, F. Palazon, M. Prato, F.D. Stasio, R. Krahne, Enhancing the performance of CdSe/CdS dot-in-rod light emitting diodes via surface ligand modification. ACS Appl. Mater. Interfaces **10**, 5665–5672 (2018). https://doi.org/10.1021/acsami.7b18780
12. W. Wondmagegn, I. Mejia, A. Salas-Villasenor, H.J. Stiegler, M.A. Quevedo-Lopez, R.J. Pieper, B.E. Gnade, CdS thin film transistor for inverter and operational amplifier circuit applications. Microelectron. Eng. **157**, 64–70 (2016). https://doi.org/10.1016/j.mee.2016.02.042
13. J.P. Enríquez, X. Mathew, Influence of the thickness on structural, optical and electrical properties of chemical bath deposited CdS thin films. Sol. Energy Mater. Sol. Cells. **76**, 313–322 (2003). https://doi.org/10.1016/S0927-0248(02)00283-0
14. H. Moualkia, S. Hariech, M.S. Aida, Structural and optical properties of CdS thin films grown by chemical bath deposition. Thin Solid Films **518**, 1259–1262 (2009). https://doi.org/10.1016/j.tsf.2009.04.067
15. N.I. Fainer, M.L. Kosinova, Y.M. Rumyantsev, E.G. Salman, F.A. Kuznetsov, Growth of PbS and CdS thin films by low-pressure chemical vapour deposition using dithiocarbamates. Thin Solid Films **280**, 16–19 (1996). https://doi.org/10.1016/0040-6090(95)08188-7
16. S. Aboul-Enein, M.H. Badawi, M. Ghali, G. Hassan, Preparation and properties of CdS thin films prepared on cold substrate as a window layer for solar cells. Renew. Energy. **14**, 113–118 (1998). https://doi.org/10.1016/S0960-1481(98)00056-1
17. D. Ellis, R.A. Berrigan, N. Maubg, S.J.C. Irvine, D.C. Hamilton, Thin films of CdTe/CdS grown by MOCVD for photovoltaics. J. Cryst. Growth **195**, 718–724 (1998). https://doi.org/10.1016/S0022-0248(98)00684-8
18. M.A. Martınez, C. Guillen, J. Herrero, Morphological and structural studies of CBD-CdS thin films by microscopy and diffraction techniques. Appl. Surf. Sci. **136**, 8–16 (1998). https://doi.org/10.1016/S0169-4332(98)00331-6
19. J.G. Vázquez-Luna, R.B. López Flores, M. Rubin-Falfán, L. Del, G. Pavón, R. Lozada-Morales, H. Juarez-Santiesteban, O. Starostenko, O. Zelaya-Angel, O. Vigil, O. Guzmán, P.D. Angel, A. González, CdSs deposited by a modified chemical-bath deposition method. J Cryst Growth **187**, 380–386 (1998). https://doi.org/10.1016/S0022-0248(97)00817-8
20. M. Khan, M.S. Khan, A. Aziz, S.A. Rahman, Z.R. Khan, Spectroscopic studies of sol-gel grown CdS nanocrystalline thin films for optoelectronic devices. Mater. Sci. Semicond. Process. **16**, 1894–1898 (2013). https://doi.org/10.1016/j.mssp.2013.07.010
21. A.A. Yadav, M.A. Barote, E.U. Masumdar, Studies on nanocrystalline cadmium sulphide (CdS) thin films deposited by spray pyrolysis. Solid State Sci. **12**, 1173–1177 (2010). https://doi.org/10.1016/j.solidstatesciences.2010.04.001
22. T. Tadokoro, S. Ohta, T. Ishiguro, Y. Ichinose, S. Kobayshi, N. Yamamoto, Growth and characterization of CdS epilayers on (100) GaAs by atomic layer epitaxy. J. Cryst. Growth. **130**, 29–36 (1993). https://doi.org/10.1016/0022-0248(93)90832-H
23. D. Boosagulla, S. Mandati, R. Allikayala, B.V. Sarada, Room temperature pulse electrodeposition of CdS thin films for application in solar cells and photoelectrochemical cells. ECS J. Solid State Sci. Technol. **7**, 440–446 (2018). https://doi.org/10.1149/2.0261808jss
24. T.I. Zubar, V.M. Fedosyuk, A.V. Trukhanov, N.N. Kovaleva, K.A. Astapovich, D.A. Vinnik, E.L. Trukhanova, A.L. Kozlovskiy, M.V. Zdorovets, A.A. Solobai, D.I. Tishkevich, S.V. Trukhanov, Control of growth mechanism of electrodeposited nanocrystalline NiFe films. J. Electrochem. Soc. **166**, 173–180 (2019). https://doi.org/10.1149/2.1001904jes
25. T. Zubar, A.V. Trukhanov, D. Vinnik, K. Astapovich, D.I. Tishkevich, E. Kaniukov, A. Kozlovskiy, M. Zdorovets, S.V. Trukhanov, The features of the growth processes and magnetic domain

structure of NiFe nano-objects. J. Phys. Chem. C **123**, 26957–26964 (2019). https://doi.org/10.1021/acs.jpcc.9b06997
26. S.H. Pawar, C.H. Bhosale, L.P. Deshmukh, Electrochemical bath deposition technique: deposition of CdS thin films. Bull. Mater. Sci. **8**, 419–422 (1986). https://doi.org/10.1007/BF02744155
27. D.I. Tishkevich, S.S. Grabchikov, L.S. Tsybulskaya, V.S. Shendyukov, S.S. Perevoznikov, S.V. Trukhanov, E.L. Trukhanova, A.V. Trukhanov, D.A. Vinnik, Electrochemical deposition regimes and critical influence of organic additives on the structure of Bi films. J. Alloys Compd. **735**, 1943–1948 (2018). https://doi.org/10.1016/j.jallcom.2017.11.329
28. A.E. Alam, W.M. Cranton, I.M. Dharmadasa, Electrodeposition of CdS thin films from cadmium acetate and ammonium thiosulphate precursors. J. Mater. Sci. Mater. Electron. **30**, 4580–4589 (2019). https://doi.org/10.1007/s10854-019-00750-1
29. D.I. Tishkevich, S.S. Grabchikov, S.B. Lastovskii, S.V. Trukhanov, T.I. Zubar, D.S. Vasin, A.V. Trukhanov, Correlation of the synthesis conditions and microstructure for Bi-based electron shields production. J. Alloys Compd. **749**, 1036–1042 (2018). https://doi.org/10.1016/j.jallcom.2018.03.288
30. U.N. Roy, L.M. Kukreja, Oriented growth of CdS nanoparticulate film with constant average particle size with thickness up to ~1 μm. J. Cryst. Growth **250**, 405–408 (2003). https://doi.org/10.1016/S0022-0248(02)02410-7
31. B.R. Sankapal, R.S. Mane, C.D. Lokhande, Deposition of CdS thin films by the successive ionic layer adsorption and reaction (SILAR) method. Mater. Res. Bull. **35**, 177–184 (2000). https://doi.org/10.1016/S0025-5408(00)00210-5
32. C.L. McCarthya, R.L. Brutchey, Solution processing of chalcogenide materials using thiol-amine "Alkahest" solvent systems. Chem. Commun. **53**, 4888–4902 (2017). https://doi.org/10.1039/C7CC02226C
33. D.H. Webber, R.L. Brutchey, Alkahest for V2VI3 chalcogenides: dissolution of nine bulk semiconductors in a diamine-dithiol solvent mixture. J. Am. Chem. Soc. **135**, 15722–15725 (2013). https://doi.org/10.1021/ja4084336
34. P.D. Antunez, D.A. Torelli, F. Yang, F.A. Rabuffetti, N.S. Lewis, R.L. Brutchey, Low temperature solution-phase deposition of SnS thin films. Chem. Mater. **26**, 5444–5446 (2014). https://doi.org/10.1021/cm503124u
35. M.A. Almessiere, Y. Slimani, H. Güngüne, A. Bayka, S.V. Trukhanov, A.V. Trukhanov, Manganese/yttrium codoped strontium nanohexaferrites: evaluation of magnetic susceptibility and Mössbauer spectra. Nanomaterials **9**, 24 (2019). https://doi.org/10.3390/nano9010024
36. M.A. Almessiere, A.V. Trukhanov, Y. Slimani, K.Y. You, S.V. Trukhanov, E.L. Trukhanova, F. Esa, A. Sadaqat, K. Chaudhary, M. Zdorovets, A. Baykal, Correlation between composition and electrodynamics properties in nanocomposites based on hard/soft ferrimagnetics with strong exchange coupling. Nanomaterials **9**, 202–213 (2019). https://doi.org/10.3390/nano9020202
37. Q. Tian, G. Wang, W. Zhao, Y. Chen, Y. Yang, L. Huang, D. Pan, Versatile and low-toxic solution approach to binary, ternary, and quaternary metal sulfide thin films and its application in $Cu_2ZnSn(S, Se)4$ solar cells. Chem. Mater. **26**, 3098–3103 (2014). https://doi.org/10.1021/cm5002412
38. M.B. Ismail, N.C. Pastor, E.P. Soler, A. Soltani, A. Othmane, A Comparative study on surface treatments in the immobilization improvement of hexahistidine-tagged protein on the indium tin oxide surface. J. Nanomed. Nanotechnol. **7**, 1000372 (2016). https://doi.org/10.4172/2157-7439.1000372
39. H.M. Gubur, R. Esen, Annealing effects on optical and crystallographic properties of CBD grown CdS films. Semicond. Sci. Technol. **18**, 647–654 (2003). https://doi.org/10.1088/0268-1242/18/7/308
40. W.J. Müller, G. Löffler, ZurKenntnis der Farbung von gefiilltem-Cadmiumsulfid. Angewandte Chemie (German Edition) **46**, 538–539 (1933)
41. W.O. Milligan, The color and crystal structure of precipitated cadmium sulfide. J. Phys. Chem. **38**, 797–800 (1934). https://doi.org/10.1021/j150357a009
42. H.A. Colorado, S.R. Dhage, H.T. Hahn, Thermo chemical stability of cadmium sulfide nanoparticles under intense pulsed light irradiation and high temperatures. Mater. Sci. Eng. B **176**, 1161–1168 (2011). https://doi.org/10.1016/j.mseb.2011.06.003
43. M. Shakouri-Araniaand, M. Salavati-Niasari, Synthesis and characterization of cadmium sulfide nanocrystals in the presence of a new sulfur source via a simple solvothermal method. New J. Chem. **38**, 1179–1185 (2014). https://doi.org/10.1039/C3NJ00996C
44. A. Bosio, G. Rosa, N. Romeo, Past, present and future of the thin film CdTe/CdS solar cells. Sol Energy (2018). https://doi.org/10.1016/j.solener.2018.01.018
45. J.C. Orlianges, C. Champeaux, P. Dutheil, A. Catherinot, T.M. Mejean, Structural, electrical and optical properties of carbon-doped CdS thin films prepared by pulsed-laser deposition. Thin Solid Films **519**, 7611–7614 (2011). https://doi.org/10.1016/j.tsf.2010.12.139
46. V.B. Sanap, B.H. Pawar, Optical study of effect of cadmium sources on nanocrystalline CdS thin films. Chalcogenide Lett. **7**, 227–231 (2010)
47. M.N. Amroun, M. Khadraoui, R. Miloua, Z. Kebbab, K. Sahraoui, Investigation on the structural, optical and electrical properties of mixed SnS_2–CdS thin films. Opt. Int. J. Light Electron. Opt. **131**, 152–164 (2017). https://doi.org/10.1016/j.ijleo.2016.11.005
48. W. Park, Photoluminescence of nanocrystalline CdS thin films prepared by chemical bath deposition. Trans. Electr. Electron. Mater. **11**, 170–173 (2010). https://doi.org/10.4313/TEEM.2010.11.4.170
49. S.V. Trukhanov, A.V. Trukhanov, S.G. Stepin, H. Szymczak, C.E. Botez, Effect of the size factor on the magnetic properties of manganite $La_{0.50}Ba_{0.50}MnO_3$. Phys. Solid State **50**, 886–893 (2008). https://doi.org/10.1134/S1063783408050144
50. S.V. Trukhanov, A.V. Trukhanov, H. Szymczak, R. Szymczak, M. Baran, Thermal stability of A-site ordered $PrBaMn_2O_6$ manganites. J. Phys. Chem. Solids **67**, 675–681 (2006). https://doi.org/10.1016/j.jpcs.2005.09.099
51. G.C. Ozcan, H.M. Gubur, S. Alpdogan, B.K. Zeyrek, The investigation of the annealing temperature for CdS cauliflower-like thin films grown by using CBD. J. Mater. Sci. Mater. Electron. **27**(11), 12148–12154 (2016). https://doi.org/10.1007/s10854-016-5368-6
52. K.K. Nanda, S.N. Sahu, Study of CdS nanocrystallites by AFM and Raman scattering spectroscopy. Appl. Surf. Sci. **119**, 50–54 (1997). https://doi.org/10.1016/S0169-4332(97)00177-3
53. K.K. Nanda, S.N. Sarangi, S.N. Sahu, S.K. Deb, S.N. Behera, Raman spectroscopy of CdS nanocrystalline semiconductors. Phys. B **262**, 31–39 (1999). https://doi.org/10.1016/S0921-4526(98)00474-8
54. D.S. Chuu, C.M. Dai, W.F. Hsieh, C.T. Tsai, Raman investigations of the surface modes of the crystallites in CdS thin films grown by pulsed laser and thermal evaporation. J. Appl. Phys. **69**, 8402–8404 (1991). https://doi.org/10.1063/1.347405
55. P. Kumar, N. Saxena, R. Chandra, V. Gupta, A. Agarwal, D. Kanjilal, Nanotwinning and structural phase transition in CdS quantum dots. Nanoscale Res. Lett. **584**, 1–7 (2012). https://doi.org/10.1186/1556-276X-7-584
56. S. Rondiya, A. Rokade, B. Gabhale, S. Pandharkar, M. Chaudhari, A. Date, M. Chaudhary, H. Pathan, S. Jadkar, Effect of bath temperature on optical and morphology properties of CdS thin films grown by chemical bath deposition. Energy Procedia **110**, 202–209 (2017). https://doi.org/10.1016/j.egypro.2017.03.128

57. R.G. Solanki, P. Rajaram, Structural, optical and morphological properties of CdS nanoparticles synthesized using hydrazine hydrate as a complexing agent. Nano-Struct. Nano-Objects **12**, 157–165 (2017). https://doi.org/10.1016/j.nanoso.2017.10.003
58. K. Manikandan, C.S. Dilip, P. Mani, J.J. Prince, Deposition and characterization of CdS nano thin film with complexing agent triethanolamine. Am. J. Eng. Appl. Sci. **8**, 318–327 (2015). https://doi.org/10.3844/ajeassp.2015.318.327
59. N. Lau, T. Tsuge, K. Sudesh, Formation of new polyhydroxyalkanoate containing 3-hydroxy-4-methylvalerate monomer in *Burkholderia* sp. Appl. Microbiol. Biotechnol. **89**, 1599–1609 (2011). https://doi.org/10.1007/s00253-011-3097-6
60. A. León, P. Reuquen, C. Garín, R. Segura, P. Vargas, P. Zapata, P.A. Orihuela, FTIR and Raman characterization of TiO_2 nanoparticles coated with polyethylene glycol as carrier for 2-methoxyestradiol. Appl. Sci. **7**, 49 (2017). https://doi.org/10.3390/app7010049
61. H.S. Mahdi, A. Parveen, S. Agrawal, A. Azam, Microstructural and optical properties of sol gel synthesized CdS nano particles using CTAB as a surfactant. AIP Conf. Proc. **1832**, 050012 (2017). https://doi.org/10.1063/1.4980245
62. R. Sahraei, S. Shahriyar, M.H.M. Ara, A. Daneshfar, N. Shokri, Preparation of nanocrystalline CdS thin films by a new chemical bath deposition route for application in solar cells as antireflection coatings. Prog. Color Color. Coat. **3**, 82–90 (2010)
63. I.O. Troyanchuk, S.V. Trukhanov, D.D. Khalyavin, H. Szymczak, Magnetic properties of anion deficit manganites $Ln_{0.55}Ba_{0.45}MnO_{3-\gamma}$ (Ln = La, Nd, Sm, Gd, $\gamma \leqslant 0.37$). J. Magn. Magn. Mater. **208**, 217–220 (2000). https://doi.org/10.1016/S0304-8853(99)00529-6
64. S.V. Trukhanov, L.S. Lobanovski, M.V. Bushinsky, V.A. Khomchenko, N.V. Pushkarev, I.O. Tyoyanchuk, A. Maignan, D. Flahaut, H. Szymczak, R. Szymczak, Influence of oxygen vacancies on the magnetic and electrical properties of $La_{1-x}Sr_xMnO_{3-x/2}$ manganites. Eur. Phys. J. B **42**, 51–61 (2004). https://doi.org/10.1140/epjb/e2004-00357-8
65. E.K. Abdelkader, H.A. Dads, S. Oucharrou, F. Walatta, H. Elaakib, L. Nkhaili, A. Narjis, A. Khalfi, K.E. Assail, A. Outzourhit, A facile route for synthesis of cadmium sulfide thin films. Thin Solid Films **664**, 66–69 (2018). https://doi.org/10.1016/j.tsf.2018.08.034
66. M.A. Islam, M.S. Hossain, M.M. Aliyu, P. Chelvanathan, Q. Huda, M.R. Karim, K. Sopian, N. Amin, Comparison of structural and optical properties of CdS thin films grown by CSVT, CBD and sputtering techniques. Energy Procedia **33**, 203–213 (2013). https://doi.org/10.1016/j.egypro.2013.05.059
67. F.R. Ahmad, A. Yakimov, R.J. Davis, J.H. Her, J.R. Cournoyer, N.M. Ayensu, Effect of thermal annealing on the properties of cadmium sulfide deposited via chemical bath deposition. Thin Solid Films **535**, 166–170 (2013). https://doi.org/10.1016/j.tsf.2012.10.085
68. H. El-Zahed, A. El-Korashy, M.A. Rahem, Effect of heat treatment on some of the optical parameters of $Cu_9Ge_{11}Te_{80}$ films. Vacuum **68**, 19–27 (2003). https://doi.org/10.1016/S0042-207X(02)00277-4
69. P.H. Jefferson, S.A. Hatfield, T.D. Veal, P.D.C. King, C.F. McConville, Bandgap and effective mass of epitaxial cadmium oxide. Appl. Phys. Lett. **92**, 022101 (2008). https://doi.org/10.1063/1.2833269
70. A. Kuddus, M.F. Rahman, S. Ahmmed, J. Hossain, A.B.M. Ismail, Role of facile synthesized V_2O_5 as hole transport layer for CdS/CdTe heterojunction solar cell: validation of simulation using experimental data. Superlattices Microstruct **132**, 106168 (2019). https://doi.org/10.1016/j.spmi.2019.106168